

# Stability and fragmentation processes of highly charged sodium clusters

G.E. Ntamack, F. Chandezon<sup>a</sup>, B. Manil<sup>b</sup>, H. Lebius, S. Tomita<sup>c</sup>, C. Guet<sup>d</sup>, M.G. Kwato Njock<sup>e</sup>, and B.A. Huber  
CIRIL, CEA-CNRS-ISMRA, Rue C. Bloch, B.P. 5133, 14070 Caen Cedex 05, France

Received 10 September 2002

Published online 3 July 2003 – © EDP Sciences, Società Italiana di Fisica, Springer-Verlag 2003

**Abstract.** Highly charged sodium clusters produced in collisions between neutral clusters and multiply charged ions are formed within a large range of temperatures and fissilities, and identified by means of a high-resolution reflectron-type time-of-flight mass spectrometer ( $m/\delta m \approx 14000$ ). The limit of stability of these charged clusters is experimentally investigated, and the time-of-flight spectra are compared with theoretical spectra based on Monte-Carlo simulations. The results indicate that the maximum fissility ( $X$ ) of stable clusters is approaching the Rayleigh limit ( $X = 1$ ) for larger clusters sizes. It is mainly limited by the initial neutral cluster temperature ( $T \approx 100$  K) and the energy transfer in the ionizing collision. In addition, the comparison between the measured and simulated spectra suggests for high cluster charges a multi-fragmentation process, in which most of charge is emitted, creating low charged residual cluster ions.

**PACS.** 36.40.Wa Charged clusters – 34.70.+e Charge transfer – 36.40.Qv Stability and fragmentation of clusters – 61.46.+w Nanoscale materials: clusters, nanoparticles, nanotubes, and nanocrystals

## 1 Introduction

The stability of complex systems depends on the strength of the intermolecular forces, on the amount of energy stored in different internal modes and in the case of small or finite-size systems on the excess of charges carried by the system. In the case of atomic clusters, the size of the object can be varied over a very large range and due to improved experimental techniques the charge state as well as the internal energy can be “controlled”. This allows a better insight into the onset of the Coulomb instabilities and the dominant decay mechanisms [1].

The Coulomb instability in finite systems results from a competition between cohesive surface energy and disruptive Coulomb energy. Lord Rayleigh was the first to study this problem theoretically in 1882 [2]. He calculated the maximum electric charge a liquid conducting drop, in the spherical equilibrium shape, can stand. In this case, the drop becomes spontaneously unstable regarding the loss of charged fragment(s) when the Coulomb energy  $E_c^{\text{sphere}}$  overcomes twice the surface energy  $E_s^{\text{sphere}}$ :

$$E_c^{\text{sphere}} \geq 2E_s^{\text{sphere}}. \quad (1)$$

<sup>a</sup> Present address: DRFMC, CEA-Grenoble, France.

<sup>b</sup> e-mail: manil@ganil.fr

<sup>c</sup> Present address: Institute of Physics and Astronomy, Aarhus, Denmark.

<sup>d</sup> Present address: DPTA, CEA-Ile de France, France.

<sup>e</sup> Present address: Center for Atomic Molecular Physics and Quantum Optics, Douala, Cameroon.

Later, on a totally different length scale and for systems where the charge is volume distributed (atomic nucleus), this competition has been quantified for the nuclear fission, within the liquid-drop model [3], by the introduction of the fissility parameter  $X$  defined as

$$X = \frac{E_c^{\text{sphere}}}{2E_s^{\text{sphere}}}. \quad (2)$$

The case  $X = 1$ , the so-called Rayleigh limit for Coulomb instability, has never been established explicitly in the experiment. Nuclear fission is usually observed for  $X < 1$  as a thermally activated process. The nucleus must overcome a barrier in order to fission, the height of which converges towards 0 as  $X$  approaches 1 [3].

For a metal cluster of size  $n$  and charge  $q$ , the equation (2) can be written as

$$X = \alpha \left( \frac{q^2}{n} \right), \quad (3)$$

where  $\alpha \approx 2.5$  for sodium (of interest in this paper) [1]. The limit  $X = 1$  corresponds to a critical size  $n_{\text{cr}}(q)$ , which depends on the charge state  $q$  of the cluster (*e.g.*,  $n_{\text{cr}} = 90$  for  $q = 6$ ). However, as in nuclei, due to the finite internal energy the systems with  $X < 1$  are metastable and the observed size limit in the measured mass spectrum, the appearance size  $n_{\text{app}}(q)$ , depends on the vibrational temperature and the experimental time scale. Moreover, when clusters are ionized in peripheral collision with highly charged ions, the excitation energy transferred

to the cluster is predicted to be very low and the stability is mainly limited by the initial cluster temperature [4, 13]. Ionization by highly charged ions allows to produce “cold” highly charged clusters in a large range of fissilities, below and well above  $X = 1$  [5]. The fissility of the prepared clusters is not limited by the competition between fission and evaporation processes as in photo-ionization experiments ( $X_{\max} \approx 0.3$  for sodium clusters ionized by laser ionization) [6, 7]. Therefore, this method opens up also the possibility to prove the validity of equation (1) and to investigate in detail the fragmentation processes of “cold” systems.

This paper is organized as follows. The experimental set-up is detailed in Section 2 and the main results are presented in Section 3. In Section 4, we discuss and compare the experimental results with simulated spectra obtained with a simulation program. Finally, conclusion follows in Section 5.

## 2 Experimental set-up

Details of the experimental apparatus are given in reference [8]. In brief, neutral sodium clusters are produced in a gas aggregation source, where condensation occurs in a atmosphere cooled with liquid nitrogen at approximately 100 K [9]. A thermostated heat bath can be added to increase the cluster temperature  $T$  [10]. A beam of neutral clusters is formed, and after passing through differential pumping stages it crosses perpendicularly a pulsed beam of multiply charged ions  $A^{z+}$ . The ionized clusters  $Na_n^{q+}$  and fragments are separated according to their size to charge ratio  $n/q$  by a high-resolution reflectron-type time-of-flight mass spectrometer. They are detected by two cascaded rectangular microchannelplates. The multi-hit detection system works in an event-by-event acquisition mode, which registers successively arrival times of all clusters which reach the detector.

The characteristic mass resolution of the reflectron-type spectrometer is  $m/\delta m \approx 14\,000$  (measured for  $Na_{100}^+$ ), which allows to identify peaks of 10-fold charged clusters as displayed in Figure 1, and to extract easily the appearance sizes for charges up to  $q = 10$ . The appearance size  $n_{\text{app}}(q)$  is determined as the threshold of the rising intensity for a  $q$ -times charged cluster (see [11] for more details).

## 3 Experimental results

The observed appearance size  $n_{\text{app}}(q)$  depends on the cluster temperature. In order to demonstrate this temperature dependence, we measured  $n_{\text{app}}(q)$  for a given projectile charge state ( $O^{5+}$ :  $E = 100$  keV,  $v \approx 0.5$  a.u.) colliding with a neutral cluster beam thermalized at different initial heat bath temperatures  $T$ , varying from 100 to 377 K. The results for the four-times charged sodium clusters are presented in Table 1. The appearance size decreases when the heat bath temperature  $T$  decreases, except at the highest

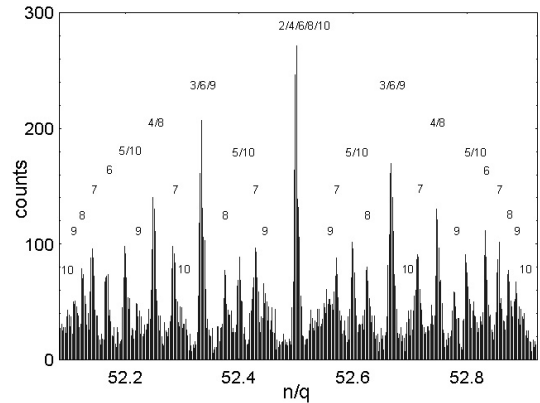


**Fig. 1.** Magnified part of a  $Na_n^{q+}$  time-of-flight mass spectrum produced in collisions with  $Xe^{28+}$  ions (kinetic energy  $E = 560$  keV, velocity  $v \approx 0.41$  a.u.). The given numbers indicate the charge state ( $q \leq 10$ ) of clusters contributing to the different peaks.

**Table 1.** Appearance size  $n_{\text{app}}$  for fourfold charged sodium clusters  $Na_n^{4+}$  as a function of the initial temperature  $T$  of the neutral clusters  $Na_n$ . The value of the appearance size at 0 K is extrapolated.

		$O^{5+} + Na_n \rightarrow Na_n^{4+}$					
$T$ (K)	0	100	223	272	326	373	
$n_{\text{app}}$	80	$82 \pm 6$	$99 \pm 5$	$104 \pm 6$	$118 \pm 2$	$117 \pm 2$	

temperatures, where  $n_{\text{app}}(q = 4)$  saturates at the value close to the laser value  $n_{\text{app}}^{\text{laser}}(q = 4) = (123 \pm 2)$  [6]. In this case, the appearance size becomes independent of the initial temperature as for larger systems the fission barrier becomes higher than the activation energy for emission of a monomer, thus favoring evaporation process. By extrapolation, we obtain the value of the appearance size at 0 K:  $n_{\text{app}}^{T=0}(q = 4) = 80$ , which corresponds to a fissility of  $X \approx 0.5$ . Moreover, using the image charge model to estimate the fission barrier height [1] and subtracting the initial cluster temperature (100 K), we estimate the energy transferred in the collision to be about 5 eV [11], in good agreement with theory [4, 13].

As the energy transferred during the ionizing collision depends on the projectile charge  $z$ , we can also vary the charged cluster temperature by changing  $z$  [4]. We performed different experiments where we used several projectiles with charges  $1 \leq z \leq 28$  and kinetic energies of  $E = 20z$  keV ( $0.3 \leq v \leq 0.5$  a.u.) [11]. The results are displayed in Figure 2. When  $z$  increases, the appearance size  $n_{\text{app}}(q \leq 7)$  decreases, in particular for low projectile charges and larger systems. This is due to the fact that the electronic excitation energy decreases with increasing projectile charge, as cluster multi-ionization occurs in collisions with larger impact parameters. At high projectile charges ( $z \geq 11$ )  $n_{\text{app}}(q)$  saturates because, in this case, the transferred vibrational energy becomes smaller than the initial internal energy corresponding to a temperature of 100 K.

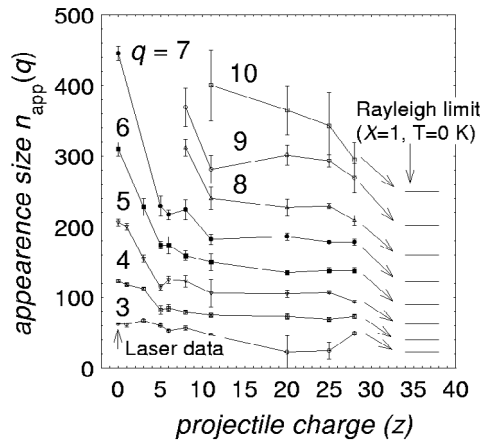


**Fig. 2.** Appearance size  $n_{\text{app}}$  of  $q$ -fold charged clusters  $\text{Na}_n^{q+}$  as a function of the projectile charge  $z$ . The data labeled “laser data” correspond to photo-ionized clusters (from Ref. [6]). On the right hand, the Rayleigh limit calculated with equation (1) is represented.

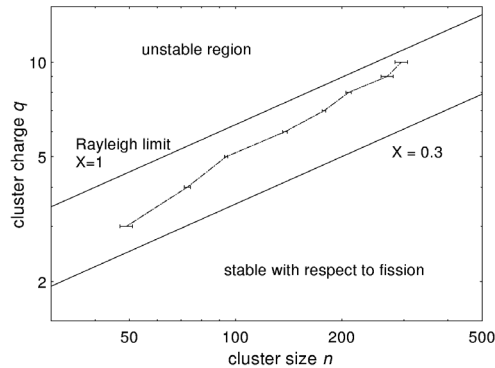


**Fig. 3.** Appearance size  $n_{\text{app}}$  of  $q$ -fold charged clusters  $\text{Na}_n^{q+}$  obtained with  $\text{Xe}^{28+}$  projectiles ( $E = 560$  keV,  $v \approx 0.41$  a.u.) in a double-log-plot of cluster charge  $q$  versus cluster size  $n$ . The lines correspond to the Rayleigh limit ( $X = 1$ ) and to the photo-ionization experiments ( $X \approx 0.3$ , see Ref. [6]).

In addition, the evolution of the measured appearance sizes with the size of the cluster is plotted in Figure 4 for  $\text{Xe}^{28+}$  projectile. The experimental values are well above the laser data corresponding to  $X \approx 0.3$ , but they are below the Rayleigh limit ( $X = 1$ ). However, they are strongly approaching the Rayleigh limit ( $X = 1$ ) for large cluster charges and sizes. The maximum fissility reached is  $X \approx (0.85 \pm 0.07)$  for  $q = 10$  and  $n = 294$ . The fact that this fissility is smaller than the value of 1 is due to the initial cluster temperature of 100 K [11], the influence of which becomes less important for larger systems.

## 4 Simulation

In order to better understand the complex time-of-flight mass spectra measured in this ion-cluster experiment and to predict its variation with different parameters like primary size distribution of the neutral clusters, the ionization probability, the energy transfer in the collision or the

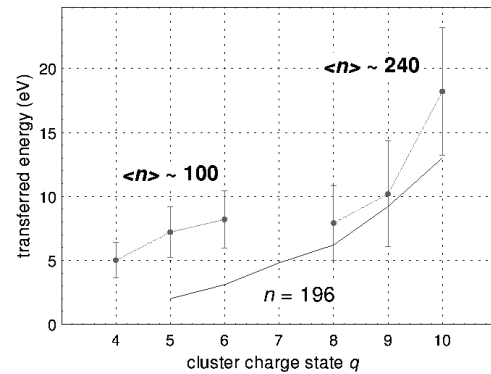


**Fig. 4.** Energy transferred in a collision with  $\text{Xe}^{28+}$  ions as a function of the cluster charge state for different mean cluster sizes. The vertical bars symbolize the Gaussian half-width of the internal energy distributions. The full line represents theoretical results, predicted by the Vlasov model for a cluster size of  $n = 196$  [4].

different decay scenarios, we have developed a Monte-Carlo code to simulate as well as the trajectories in the time-of-flight spectrometer allowing for different decay processes. More details can be found in the reference [12].

In brief, the simulation program determines in the beginning by a random number generator the cluster size  $n$  and charge  $q$  according to the size distribution and the experimentally determined ionization probabilities. Depending on the fissility of the resulting cluster ion, three different possible decay processes are taken into account: fission, evaporation or multi-fragmentation. The corresponding decay rates are calculated with a statistical model. In the second part, the time-of-flight is calculated and the mass spectra are constructed.

The appearance size in a given charge state as well the evolution of the intensity close to it, are rather sensitive to the internal energy of the system. In order to describe the increase of the intensity with the cluster size  $n$  after the threshold, contributions from different processes have to be taken into account: either  $q$ -fold charged clusters, which are formed directly in the collisions and which are stable during the time-of-flight, or clusters in higher charge states ( $q + 1$  or  $q + 2$ ) which decay by asymmetric fission into the final charge state  $q$ . By using the corresponding relative ionization cross sections and by varying the internal energy distributions (approximated by Gaussian distribution), we can extract the transferred energy after subtracting the initial internal energy [12]. The results, for  $q = 4$  and  $q = 8$  with sizes close to the threshold  $n \sim 100$  and  $n \sim 240$  [11], are presented in Figure 4 and compared with theoretical predictions obtained by solving the Vlasov equation [4]. The extracted values show a similar behavior as the theoretical predictions. In order to create higher charge states, the collision occurs at smaller impact parameters leading to a stronger electronic excitation.

A magnified part of simulated time-of-flight spectrum is shown in Figure 5. It is obtained by using the energy distribution represented Figure 4. The comparison with

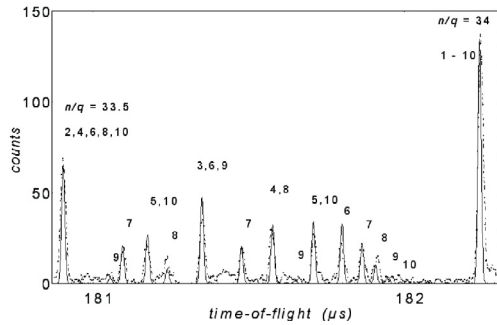
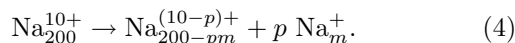


**Fig. 5.** Comparison between a magnified part ( $33.5 \leq n/q \leq 34$ ) of the simulated (full line) and the experimental (dots) time-of-flight spectrum. The given numbers indicate the charge states of different cluster ions.

the experimental spectrum yields a satisfying agreement. Some deviations in the peak heights might be explained by the limited statistics of the experimental and simulated spectra. However, a closer inspection demonstrates that several parts of the experimental spectrum can not be reproduced by the simulation. Those parts are due to evaporation processes of clusters in low charge states. However, the internal energy assumed in this simulation for the low charge state ions is not sufficient to provoke such a high evaporation rate [12].

An example is shown in Figure 6. Close to clusters characterized by  $n/q = 24$  two small contributions are observed which correspond to  $\text{Na}_{73}^{3+}$  and  $\text{Na}_{49}^{2+}$ , which have emitted during the first drift region of the time-of-flight system a single monomer. This implies that the internal energies of these ions must be larger than 15 eV, much larger than the values expected from the simulation ( $\leq 5$  eV). Due to the fact, that these contributions are not showing up in the simulation, which only took into account charge states up to 10, and by considering the result in Figure 4, we suggest that these clusters have been formed initially in charge states higher than 10. We propose the following decay scenario: in a first step, highly charged cluster ions are formed with a high fissility parameter ( $X > 1$  and  $q > 10$ ). In a second step, they decay instantaneously by emitting  $p$  small singly charged fragments, forming “hot” residual cluster ions in low charge state as:



Finally, the hot residues are evaporating in the first time-of-flight region. This hypothesis is supported by calculations of the  $Q$ -value of the process, defined as energy difference between the initial and final state [1]. These calculations clearly demonstrate that the potential energy minimum favors the emission of 7 or 8 singly charged dimers or trimers forming a residual ion in charge state 2 or 3 [12], which are observed in the experimental spectra.

## 5 Conclusion

We have measured the appearance size  $n_{\text{app}}(q)$  of multiply charged sodium clusters ( $\text{Na}_n^{q+}$ ) formed in collisions

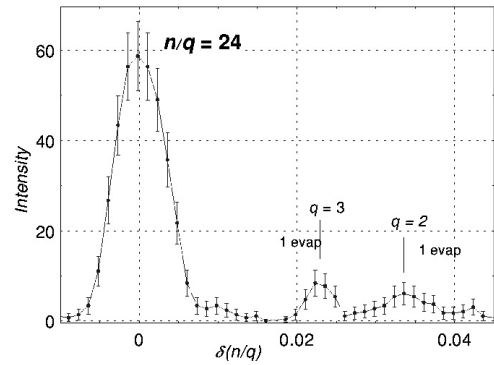


**Fig. 6.** Magnified part of an experimental time-of-flight spectrum in the range between  $n/q = 23.99$  and  $n/q = 24.045$ . The vertical bars indicate the positions of clusters  $\text{Na}_{73}^{3+}$  and  $\text{Na}_{49}^{2+}$ , which have emitted during the first drift region of the time-of-flight system a single monomer.

of “cold” neutral clusters with low energy highly charged ions ( $z \leq 28$ ). The measured appearance sizes are well below those obtained by laser ionization but they are still above the critical values as predicted by Lord Rayleigh. This is due to the internal energy of the ionized clusters. However, the temperature effect becomes less important for larger systems, thus we approach the Rayleigh limit with increasing size and charge of the cluster. The maximum fissility observed in the experiment is  $X = 0.85$  for the system  $\text{Na}_{294}^{10+}$ . The comparison of experimental with simulated spectra allows to determine the internal energy distribution of the ionized clusters. The obtained values increase with the cluster charge state and show good agreement with theoretical predictions. Furthermore, the analysis of the spectra suggest that for systems with  $X > 1$  a decay mechanism exist, where most of the charges are lost in the collective emission of many small singly charged fragments creating a residual ions in low charge states ( $q = 2$  or 3).

## References

1. U. Näher *et al.*, Phys. Rep. **285**, 245 (1997)
2. Lord Rayleigh, Phil. Mag. **14**, 185 (1882)
3. N. Bohr, J.A. Wheeler, Phys. Rev. **56**, 426 (1939)
4. L. Plagne, C. Guet, Phys. Rev. A **59**, 4461 (1999)
5. C. Guet *et al.*, Z. Phys. D **40**, 317 (1997)
6. T.P. Martin *et al.*, Chem. Phys. Lett. **196**, 113 (1992); U. Näher *et al.*, Z. Phys. D **31**, 191 (1994)
7. C. Bréchnac *et al.*, Phys. Rev. B **49**, 2825 (1994)
8. T. Bergen *et al.*, Rev. Sci. Instrum. **70**, 3244 (1999)
9. C. Ellert *et al.*, Phys. Rev. Lett. **75**, 1731 (1995)
10. F. Chandezon *et al.*, Chem. Phys. Lett. **277**, 450 (1997); J. Borggreen *et al.*, Eur. Phys. J. D **9**, 119 (1999)
11. F. Chandezon *et al.*, Phys. Rev. Lett. **87**, 153402 (2001)
12. G.E. Ntamack *et al.*, J. Phys. B **35**, 2729 (2002)
13. S. Daligault *et al.*, Phys. Rev. A (to be published)